



UNIVERSITI PUTRA MALAYSIA

**MICROSTRUCTURE AND DYNAMIC MAGNETIC PROPERTIES OF
THALLIUM-BASED SUPERCONDUCTORS**

ABDUL TALIB BIN SHAARI

FSAS 2002 54

**MICROSTRUCTURE AND DYNAMIC MAGNETIC PROPERTIES OF
THALLIUM-BASED SUPERCONDUCTORS**

ABDUL TALIB BIN SHAARI

**MASTER OF SCIENCE
UNIVERSITI PUTRA MALAYSIA**

2002



**MICROSTRUCTURE AND DYNAMIC MAGNETIC PROPERTIES OF
THALLIUM-BASED SUPERCONDUCTORS**

By

ABDUL TALIB BIN SHAARI

**Thesis Submitted to the School of Graduate Studies, Universiti Putra Malaysia,
in Fulfilment of the Requirement for the degree of Master of Science**

July 2002



Abstract of the thesis presented to the Senate of Universiti Putra Malaysia in fulfillment of the requirements for the degree of Master of Science

MICROSTRUCTURE AND DYNAMIC MAGNETIC PROPERTIES OF THALLIUM-BASED SUPERCONDUCTORS

By

ABDUL TALIB BIN SHAARI

July 2002

Chairman: Professor Dr. Abdul Halim Shaari
Faculty: Science and Environmental Studies

Ac susceptibility study is one of the best methods in characterizing bulk superconductors. Four systems (A, B, C and D) of Thallium-based bulk superconductors were analyzed using this method. They were A = $(\text{Tl}_{0.85}\text{Cr}_{0.15}) \text{Sr}_2 (\text{Ca}_{1-x}\text{Pr}_x) \text{Cu}_2\text{O}_7$, B = $(\text{Tl}_{0.85}\text{Cr}_{0.15}) \text{Sr}_2 (\text{Ca}_{1-x}\text{Nd}_x) \text{Cu}_2\text{O}_7$, C = $(\text{Tl}_{0.85}\text{Cr}_{0.15}) \text{Sr}_2 (\text{Ca}_{1-x}\text{Pr}_x) \text{Cu}_2\text{O}_7$, and D = $(\text{Tl}_{0.85}\text{Cr}_{0.15}) \text{Sr}_2 (\text{Sr}_{1-x}\text{Pr}_x) \text{Cu}_2\text{O}_7$. The temperature dependent ac susceptibility curves and field dependent ac susceptibility curves were obtained using Lake Shore AC Susceptometer Model 7000. The dimensions of each sample were 2mmx2mmx10mm. Certain ranges of temperatures were identified from temperature dependent ac susceptibility curves for use in plotting the field dependent ac susceptibility curves for each sample. The applied fields (0.1 – 10 Oersted) were not high enough to observe the contributions from intragranular supercurrents. Therefore the data obtained were from the intergranular matrix. Bean's Model is used to explain the dynamic magnetic properties that resulted from the data T_c , T_p and T_{c_j} that were obtained from temperature dependent ac susceptibility curves. I_0 was calculated from T_c and T_{c_j} using the Ambegaokar-Baratoff formula and $J_c(T)$ were



calculated from Bean's model. T_c and I_0 were plotted against the concentration x and $J_c(T)$ were plotted against temperature T .

From this research work the effect of doping in general reduced the T_c and I_0 values. For system D, the values fall gradually where as for the rest they fall very fast especially those of system B. These are reflected in the graphs of T_c versus x and I_0 versus x . The degree of compactness can be drawn as follows: $D > C > A > B$.

From $J_c(T)$ versus T , $J_c(T)$ values drop gradually for system D whereas for the other systems, $J_c(T)$ values drop very fast. All the $J_c(T)$ maximum values were increased as the field increased and these were attained at lower temperatures. At particular field, as the concentration increased, these were attained at lower temperatures also.

Kim's Model was used to explain the data obtained from field dependent ac susceptibility curves. It was found that systems D and C have certain range of temperatures where the curves follow Kim's Model. For example, these are reflected in the curves $\chi_m''(H_m)$ versus $-\chi_m'(H_m)$ and $\chi_m''(H_m)$ versus $\log H_m$ at various temperatures and dopings for system D, $x = 0.3$, $T = 59$ K, $J_c(H) = 2.66 \times 10^5 \text{ Am}^{-2}$, for system C, $x = 0.2$, $T = 70$ K, $J_c(H) = 1.66 \times 10^5 \text{ Am}^{-2}$ and for system A, $x = 0.2$, $T = 53$ K, $J_c(H) = 3.46 \times 10^5 \text{ Am}^{-2}$.

SEM photographs were also taken and analyzed. The microstructures of systems A and B are more flat and round in shape. They look porous and having bigger voids whereas those of systems D and C have long rectangular shape or rod-

liked in shape and look more compact and homogenous. The compactness and small voids probably lead to slow reduction of I_0 and T_c in systems D and C. Thus systems D and C are better connected than those of Systems A and B.

Thus the doping and heat treatment have certain effects on the dynamic magnetic properties of these superconductors as shown in the values of the critical current density $J_c(T)$, $J_c(H)$, I_0 and T_c . Further heating (1.5 hours), as in system A, did not strengthen the weak-links.

From the analysis of data obtained from temperature dependent ac susceptibility curves, analysis of the field dependent ac susceptibility curves and the analysis of the SEM photographs, system D, $x = 0.3$ is believed to have the best microstructure that give the dynamic magnetic properties which can be explained by the Bean's Model and Kim's Model.

Abstrak tesis yang dikemukakan kepada Senat Universiti Putra Malaysia bagi memenuhi keperluan ijazah Master Sains

**PENYELIDIKAN MIKROSTRUKTUR DAN CIRI-CIRI DINAMIK
KEMAGNETAN BAGI BAHAN SUPERKONDUCTOR
BERASASKAN THALLIUM**

Oleh

ABDUL TALIB BIN SHAARI

Julai 2002

Pengerusi: Profesor Dr. Abdul Halim Shaari
Fakulti: Sains dan Pengajian Alam Sekitar

Penyelidikan kerentanan au adalah salah satu cara yang terbaik untuk mengkaji ciri-ciri kemagnetan bahan superkonduktor. Empat sistem superkonduktor berasaskan Thallium (Sistem A, B, C and D) telah dikaji menggunakan teknik ini. Empat system itu ialah sebagai berikut: A = $(\text{Tl}_{0.85}\text{Cr}_{0.15}) \text{Sr}_2 (\text{Ca}_{1-x}\text{Pr}_x) \text{Cu}_2\text{O}_7$, B = $(\text{Tl}_{0.85}\text{Cr}_{0.15}) \text{Sr}_2 (\text{Ca}_{1-x}\text{Nd}_x) \text{Cu}_2\text{O}_7$, C = $(\text{Tl}_{0.85}\text{Cr}_{0.15}) \text{Sr}_2 \text{Ca}_{1-x}\text{Pr}_x \text{Cu}_2\text{O}_7$, D = $(\text{Tl}_{0.85}\text{Cr}_{0.15}) \text{Sr}_2 (\text{Sr}_{1-x}\text{Pr}_x) \text{Cu}_2\text{O}_7$. Graf kerentanan au yang bergantung kepada suhu dan bergantung pada medan didapati menggunakan alat A.C. Susceptometer Model 7000. Julat suhu dipilih dari graf kerentanan au bergantung kepada suhu untuk digunakan melakar graf kerentanan au bergantung kepada medan. Dimensi sampel ialah 2mm x 2mm x 10mm. Mikrostruktur tiap sampel diambil dengan menggunakan alat SEM. Daripada graf kerentanan au bergantung pada medan, julat suhu yang mengikuti tuntutan model keadaan genting (Kim's Model) telah dipilih. Data yang akan didapati adalah dari matriks antaragranular. Model Bean digunakan untuk menganalisis data dari graf



kerentanan au bergantung pada suhu. I_0 dihasilkan dengan menggunakan formula Ambegaokar-Baratoff dengan menggunakan T_c dan T_{c_j} yang didapati dari graf kerentanan au bergantung kepada suhu dan $J_c(T)$ dikira dari Model Bean. Suhu T_c dan I_0 diplotkan melawan x dan $J_c(T)$ diplotkan melawan suhu T .

Daripada penyelidikan ini akibat daripada pendopan, T_c dan I_0 telah menurun nilainya. Bagi sampel D nilai ini menurun dengan perlahan tetapi bagi sistem yang lain nilai ini menurun dengan cepat. Ini menunjukkan bahawa sistem D mempunyai mikrostruktur yang padat dari yang lain. Kepadatan itu boleh ditulis sebagai berikut: $D > C > A > B$.

Daripada Graf $J_c(T)$ melawan T , $J_c(T)$ menurun secara perlahan juga bagi sistem D. Sistem lain menurun dengan cepat terutama sistem B. Semua nilai maxima $J_c(T)$ meningkat bila medan bertambah tetapi pada suhu rendah. Pada nilai medan tertentu, nilai $J_c(T)$ bertambah bila x bertambah tetapi pada suhu rendah juga.

Model Kim digunakan untuk menganalisis data daripada graf bergantung pada medan. Juga didapati bahawa sistem D dan C mempunyai julat suhu lebih besar yang memenuhi tuntutan Model Kim. Ini boleh dilihat pada graf $\chi_m''(H_m)$ melawan $-\chi_m'$ (H_m) dan graf $\chi_m''(H_m)$ melawan $\log H_m$ untuk sistem D, $x = 0.3$, $T = 59$ K, $J_c(H) = 2.66 \times 10^5 \text{ Am}^{-2}$, untuk sistem C, $x = 0.2$, $T = 70$ K, $J_c(H) = 1.66 \times 10^5 \text{ Am}^{-2}$ dan sistem A, $x = 0.2$, $T = 53$ K, $J_c(H) = 3.46 \times 10^5 \text{ Am}^{-2}$.

Gambar SEM juga diambil bagi semua sampel dan dianalisis. Didapati mikrostruktur bagi sistem A dan B bulat, besar dan leper, tetapi bagi sistem

D dan C condong kepada bentuk segiempat panjang dan kecil. Mikrostruktur sistem D dan C nampak lebih padat daripada sistem A dan B. Mungkin kepadatan ini menyebabkan nilai T_c dan nilai I_0 menurun lebih lambat berbanding dengan sistem A dan B.

Nampaknya pendopan ada kesan kepada nilai $J_c(T)$, $J_c(H)$, I_0 dan T_c tetapi pemanasan lebih (1.5 jam) tidak memberi kesan kepada nilai nilai ini terutama pada nilai I_0 .

Daripada analisis data daripada kerentanan au bergantung pada suhu dan yang bergantung pada medan dan analisis mikrostruktur dari gambar SEM, dibuat kesimpulan bahawa sistem D, $x = 0.3$ adalah sistem yang mempunyai mikrostruktur yang terbaik yang mempunyai ciri ciri kemagnetan dinamik yang boleh diterangkan dengan menggunakan Model Bean dan Model Kim.

ACKNOWLEDGEMENTS

First and foremost, I would like to acknowledge my supervisor, Professor Dr. Abdul Halim Shaari , for giving me the opportunity to pursue my master's degree under his supervision and also to Associate Professor Dr. Wan Mahmood Mat Yunus and Associate Professor Dr. Jamil Suradi from Physics Department, Faculty of Science and Environmental Studies, UPM as members of the Examination Committee. Special thanks to Professor Dr. Roslan Abdul Shukor from UKM for providing the thallium-based superconductor samples for my ac susceptibility and SEM studies and to Dr. S.B.Mohamed who is now at Tsukuba University, Tokyo, Japan and Dr. Azhan Hashim, who is now at UiTM, Jengka, Pahang for their valueable discussions and helps during my course of experiments Also I would like to thank En. Lim Kean Pah, Kabashi, A.I.Malik, Koh Soog Foo, Yu Ong Sing, Abdul Halim Baijan, Abdullah Cik, Imad, Pn. Iftetan, Ari , Huda Abdullah, Teh Jio Yew and Cik Sharmiwati Mohd. Shariff for their helps in using the computers and other instruments in the laboratory.

Particular thanks are also owed to En.Razak Harun for his help in the usage of instruments in the laboratory and to Cik Suleka Madhavan, Cik Azilah Abdul Jalil and Encik Ho Oi Kuan, for their helps in preparing the samples and the use of SEM instruments and to Encik Baharuddin Ibrahim and Encik Zulambiar Bahari from Multimedia Laboratory for helping me in using the Scanner.



This thesis submitted to the Senate of Universiti Putra Malaysia has been accepted as fulfillment of the requirements for the degree of Master of Science. The members of the Supervisory Committee are as follows:

ABDUL HALIM SHAARI, Ph.D.

Professor
Faculty of Science and Environmental Studies
Universiti Putra Malaysia
(Chaiman)

WAN MAHMOOD MAT YUNUS, Ph.D.

Associate Professor
Faculty of Science and Environmental Studies
Universiti Putra Malaysia
(Member)

JAMIL SURADI, Ph.D.

Associate Professor
Faculty of Science and Environmental Studies
Universiti Putra Malaysia
(Member)

AINI IDERIS, Ph.D.

Professor/ Dean,
School of Graduate Studies
Universiti Putra Malaysia

Date:



TABLE OF CONTENTS

	Page
ABSTRACT	.ii
ABSTRAK	v
ACNOWLEDGEMENT	viii
APPROVAL SHEET	ix
APPROVAL SHEET	x
DECLARATION FORM	xi
LIST OF TABLES	xiv
LIST OF FIGURES	xv
LIST OF ABBREVIATIONS	xix
CHAPTERS	
I GENERAL INTRODUCTION	
Introduction	1
High T_c Superconductors	3
Thallium-based High T_c Superconductors	3
Magnetic Response of High T_c Superconductors	8
Objectives of Research	10
Thesis content	11
II LITERATURE REVIEW	
Introduction	12
Ac Susceptibilities and SEM Measurements of Superconductors	12
J_c Determination Using Bean's and Kim's Model	36
III THEORY	
Introduction	42
Theory of Ac Susceptibility	42
Magnetic System	43
Critical Current Density	47
Bean's Model	48
Kim's Model	50
The Determination of J_c	52
Theoretical Model For Granularity	59
IV METHODOLOGY	
Introduction	66
Ac Susceptometry	67
Scanning Electron Microscopy	70



V	RESULTS AND DISCUSSIONS	
	Introduction	73
	Section A: Analysis for temperature dependence ac susceptibility curves	74
	Section B: Analysis of graphs plotted from data obtained from temperature dependent ac susceptibility curves.	86
	Section C: Analysis for field dependence ac susceptibility curves	96
	Section D: Analysis for SEM micrographs	116
	Section E: Observations	129
VI	CONCLUSION AND SUGGESTION	132
	Conclusion and Suggestion	132
	REFERENCES	135
	APPENDICES	139
	BIODATA	149



LIST OF TABLES

Table		Page
1.1	TlBaCaCuO System	5
5.1	Formulae Of System A, B, C And D	73
5.2	Data $J_c(T)$ From Temperature Dependent Ac Susceptibility Curves	89
5.3	Data obtained From Temperature Dependent Ac Susceptibility Curve	90
5.4	Temperatures Ranges For Field Dependent Curves (Kim's Model)	97
5.5	Data Obtained From Field Dependent Ac Susceptibility Curves	98
5.6	Data $J_c(H_i)$ Obtained From Field Dependent Ac Susceptibility Curves	99



LIST OF FIGURES

Figure		Page
1.1	Effects of field cooling (ZFC) and field cooling (FC) on superconductor	2
1.2	The schematic representation of mono-and bi-layered Tl-based cuprates	7
3.1	An experimental arrangement used in an AC Susceptometer	53
3.2	Magnetization curve showing an ac measurement	53
3.3	The graph of χ'' versus χ' (Argan Diagram)	54
3.4	The graph of χ'' versus $-\chi'$ (Bean's model)	54
3.5	The graph of χ'' versus $-\chi'$ (Kim's model)	54
3.6	Local internal field distributions	55
3.7	Critical current density (Bean's model) for internal field of 3.6	55
3.8	Critical current density (Kim's model) for internal field of 3.6	56
3.9	Ac susceptibility curves (Bean's model)	56
3.10	Bean's model of critical current density, J_c (T)	57
3.11	Ac susceptibility curves (Kim's model)	57
3.12	Kim's model of critical current density, $J_c(H_i)$	58
3.13	Magnetization curves based on the Bean critical state model	58
3.14	Josephson vortices and Abrikosov vortices	64
3.15	Intergranular flux line pinning sites	65
3.16	Slab geometry of YBCO sample	65
4.1	Ac Susceptometer	71
4.2	Scanning Electron Microscope Model JSN 6400	72
5.1	Temperature dependence ac susceptibility curves	78
5.1a	System A, $x = 0$	78

5.1b	System A, $x = 0.1$	78
5.1c	System A, $x = 0.2$	79
5.1d	System A, $x = 0.3$	79
5.1e	System A, $x = 0.4$	80
5.2a	System B, $x = 0.1$	80
5.2b	System B, $x = 0.2$	81
5.2c	System B, $x = 0.3$	81
5.3a	System C, $x = 0$	82
5.3b	System C, $x = 0.1$	82
5.3c	System C, $x = 0.2$	83
5.3d	System C, $x = 0.3$	83
5.3e	System C, $x = 0.4$	84
5.4a	System D, $x = 0$	84
5.4b	System D, $x = 0.2$	85
5.4c	System D, $x = 0.3$	85
5.4d	System D, $x = 0.4$	86
	Graphs Related To ac (T) susceptibility curves	91
5.5	System A, (a) J_c vs T_p (b) T_p vs H_m (c) I_0 vs x (d) T_c vs x	91
5.6	System B, (a) J_c vs T_p (b) T_p vs H_m (c) I_0 vs x (d) T_c vs x	92
5.7	System C, (a) J_c vs T_p (b) T_p vs H_m (c) I_0 vs x (d) T_c vs x	93
5.8	System D, (a) J_c vs T_p (b) T_p vs H_m (c) I_0 vs x (d) T_c vs x	94
5.9	Comparison of Graphs of T_c of System A, B and D with System C	95
5.10	Comparison of Graphs of I_0 of System A, B and D with System C	95
5.11	Field Dependent Ac Susceptibility Curves	100
5.11	System A, $x = 0.1, T = 70$ K	100

5.12	System A, $x = 0.2, T = 50$ K	101
5.13	System A, $x = 0.2, T = 53$ K	102
5.14	System A, $x = 0.3, T = 69$ K	103
5.15	System B, $x = 0.2, T = 69$ K	104
5.16	System C, $x = 0.1, T = 89$ K	105
5.17	System C, $x = 0.2, T = 70$ K	106
5.18	System C, $x = 0.2, T = 72$ K	107
5.19	System C, $x = 0.3, T = 55$ K	108
5.20	System D, $x = 0.2, T = 59$ K	109
5.21	System D, $x = 0.2, T = 60$ K	110
5.22	System D, $x = 0.2, T = 61$ K	111
5.23	System D, $x = 0.3, T = 59$ K	112
5.24	System D, $x = 0.3, T = 60$ K	113
5.25	System D, $x = 0.3, T = 61$ K	114
5.26	System D, $x = 0.4, T = 47$ K	115
5.27a	SEM Micrograph, System A, $x = 0$	117
5.27b	SEM Micrograph, System A, $x = 0.1$	117
5.27c	SEM Micrograph, System A, $x = 0.2$	118
5.27d	SEM Micrograph, System A, $x = 0.3$	118
5.27e	SEM Micrograph, System A, $x = 0.4$	119
5.28a	SEM Micrograph, System B, $x = 0.1$	120
5.28b	SEM Micrograph, System B, $x = 0.2$	120
5.28c	SEM Micrograph, System B, $x = 0.3$	121
5.28d	SEM Micrograph, System B, $x = 0.4$	121
5.28e	SEM Micrograph, System B, $x = 0.5$	122



5.29a	SEM Micrograph, System C, $x = 0$	123
5.29b	SEM Micrograph, System C, $x = 0.1$	123
5.29c	SEM Micrograph, System C, $x = 0.2$	124
5.29d	SEM Micrograph, System C, $x = 0.3$	124
5.29e	SEM Micrograph, System C, $x = 0.4$	125
5.30a	SEM Micrograph, System D, $x = 0$	126
5.30b	SEM Micrograph, System D, $x = 0.2$	126
5.30c	SEM Micrograph, System D, $x = 0.3$	127
5.30d	SEM Micrograph, System D, $x = 0.4$	127



LIST OF ABBREVIATIONS

T_c	critical temperature of temperature dependent ac susceptibility curve
T_p	peak temperature of temperature dependent ac susceptibility curve
T_{cj}	phase lock temperature of temperature dependent ac susceptibility curve
T_{p0}	peak temperature for $x = 0$
T_{p1}	peak temperature for $x = 0.1$
T_{p2}	peak temperature for $x = 0.2$
T_{p3}	peak temperature for $x = 0.3$
T_{p4}	peak temperature for $x = 0.4$
J_c	critical current density
x	doping concentration
I_0	maximum Josephson current
E_j	Josephson coupling energy
H	magnetic field
H_i	internal magnetic field
H_m	maximum external magnetic field
H_p	external penetration field
B	magnetic induction
M	magnetization
M_l	local magnetization
HTS	high temperature superconductors
H_{ac}	applied magnetic field
m	moment
V	Voltage
χ_{ac}	ac susceptibility



μ_0	permeability of free space
a	dimension of half of slab thickness
χ_m''	intergranular matrix component of imaginary ac susceptibility
χ_m'	intergranular matrix component of real ac susceptibility
χ''	imaginary component of ac susceptibility
χ'	real component of ac susceptibility
f_g	volume fractions of superconducting grains
M_g	magnetization of superconducting grains
M_m	magnetization of intergranular matrix
χ_g	ac susceptibility of superconducting grains
H_{c1}	Lower critical magnetic field
H_{c2}	higher critical magnetic field
H_{c1g}	lower critical magnetic field of grains
k	positive constant in Kim Model
H_0	constant magnetic field in Kim Model
p	constant in Kim Model
f	frequency
c	calibration coefficient
θ	temperature
ρ	resistivity
YBCO	Yttrium Barium Copper Oxide
BSCCO	Bismuth Strontium Cobalt Copper Oxide
TBCCO	Thallium Bismuth Cobalt Copper Oxide

CHAPTER I

GENERAL INTRODUCTION.

What is a superconductor? It is a material which exhibits two distinct properties, that is, zero resistivity: $\rho = 0$ for all $T < T_c$ and zero magnetic induction: $B = 0$ inside the superconductor. The magnetic inductance becomes zero inside the superconductor when it is cooled below T_c in a weak external magnetic field. The magnetic flux is expelled from the interior of the superconductor. This effect is called the Meissner-Ochsenfeld effect after its discoverers.

In 1957, Alexei Abrikosov studied the behaviour of superconductors in an external magnetic field and found that there are two types of superconductors: Type-I and Type-II superconductors. Type-I expelled magnetic flux completely from their interior while Type-II do it completely only at small fields but partially at higher fields. Thanks to this property, i.e., the formation of the so-called mixed state, this Type-II can sustain superconductivity even in fields higher than 10 Tesla. Because of this, Type-II superconductors are of interest for most large-scale application.

In zero field cooled (ZFC) condition (See Figure 1.1), the superconductor is cooled first below T_c and when the field is applied below T_c , the field is excluded. This is called **magnetic shielding**. But in field cooled (FC) condition (See Figure 1.1) when constant field is applied before it is cooled below T_c and when it is cooled



below T_c , while the field is kept constant, the field is expelled and this called the **Meissner effect**.

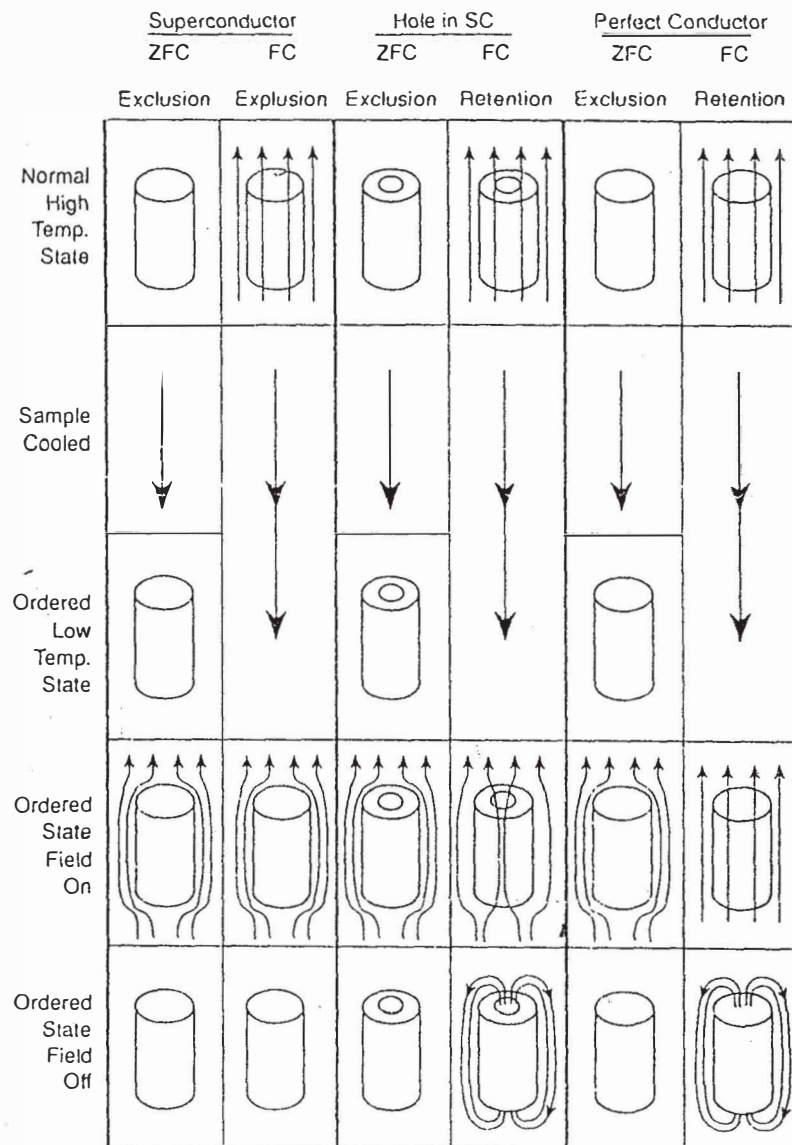


Figure 1.1: Effect of zero field cooling (ZFC) and field cooling (FC) On a superconductor.
 (Source: Superconductivity; Charles P. Poole, Jr, Academic Press, 1995)

High T_c Superconductors

High T_c superconductors belong to Type-II superconductors. Examples of high T_c superconductors are YBCO, BSCCO, TBCCO and finally HBCCO systems. The highest T_c for YBCO system belongs to YBCO (123) phase, that is, $T_c = 92$ K, while for BSCCO (2223), $T_c = 110$ K, and lastly for TBCCO (2223) and HBCCO (1223) $T_c = 125$ K and $T_c = 153$ K respectively. These High T_c superconductors are usually granular and since it is granular the problems of weak-links occur.

Thallium-Based High T_c Superconductors

Thallium-based system (Figure 1.2 and Table 1.1) was discovered by Z.Z.Sheng and A.M.Hermann (1988). TlBaCuO has $T_c = 81$ K and it rose to 100 K when Ca was included in the system and in 1993, Tl-2223 was discovered with the highest $T_c = 125$ K (Table 1.1). Thallium-based systems are considered today as the most likely candidates for power applications such as transmission lines and various magnetic systems since they have low flux creep. The thallium single layer materials such as Tl-1223 show less flux creep than the more anisotropic double layer such as Bi-2212, Bi-2223 and Tl-2223. The insulator thickness, the spacing between the copper oxide layer blocks is an important parameter for flux creep. Among the materials of the Tl-based group the best position of the irreversibility line belongs to this Tl-1223 phase. It is accepted that stronger coupling between conducting Cu-O planes separated by single-layer insulating Tl-O plane is responsible for the improved properties of this kind of material in higher magnetic fields. These types of applications requires J_c values in the range of 10^4 - 10^5 A cm⁻² which are

